Sains Malaysiana 51(8)(2022): 2473-2493
http://doi.org/10.17576/jsm-2022-5108-11

Mesoporous Silica Nanoparticle-Templated Ionic Liquid as a Drug Carrier for Ibuprofen and Quercetin

(Nanozarah Silika Mesoliang Templat Cecair Ion sebagai Pembawa Ubat untuk Ibuprofen dan Kuersetin)

NAJIHAH RAMELI[1], KHAIRULAZHAR JUMBRI[1,2,*], ANITA RAMLI[1], ROSWANIRA ABDUL WAHAB[3], HASLINA AHMAD[4] & MOHD BASYARUDDIN ABDUL RAHMAN[4]

[1]*Department of Fundamental and Applied Sciences, Universiti Teknologi Petronas, 32610 Seri Iskandar, Perak Darul Ridzuan, Malaysia*
[2]*Centre of Research in Ionic Liquids (CORIL), Universiti Teknologi PETRONAS (UTP), Bandar Seri Iskandar, Perak Darul Ridzuan, Malaysia*
[3]*Department of Chemistry, Faculty of Science, Universiti Teknologi Malaysia (UTM), 81310 Skudai, Johor Bahru, Johor Darul Takzim, Malaysia*
[4]*Department of Chemistry, Faculty of Science, Universiti Putra Malaysia, 43400 UPM Serdang, Selangor Darul Ehsan, Malaysia*

Received: 13 December 2021/Accepted: 4 March 2022

ABSTRACT

In this study, a series of mesoporous silica nanoparticle (MSN) was successfully synthesized using different ionic liquids (ILs) as a template. Five ILs and a surfactant with different alkyl side chains and types of anion namely 1-dodecyl-3-methylimidazolium iodide ([C_{12}mim][I]), 3-diethylamino propanol vanillate (DV), 2-butylamino ethanol salicylate (BS), 3-diethylamino propanol salicylate (DS), 1-butyl-3-methylimidazolium bis(trifluoromethylsulfonyl) imide ([bmim][NTf_2]) and hexadecyltrimethylammonium bromide (CTAB) were used. All MSNs produced have broad peaks, indicating mesoporous silica in amorphous form as observed by XRD while the morphology of MSN showed the agglomeration of particles and due to parallel arrangement pores size in both for FESEM and HRTEM. The MSNs are amorphous and displayed Type IV BET isotherm with H_2 hysteresis loops which is a typical isotherm for mesoporous materials and the highest surface area obtained was 638 m^2/g. The study on uptake and release of ibuprofen and quercetin were carried out, where ibuprofen showed higher drug uptake compared to quercetin due to better interaction of MSN with drug molecules. The drug release conducted at 48 h indicates 33.1% of ibuprofen and 38.4% quercetin released. It can be indicated that MSN-BS is the best for drug loading and release. Drugs release kinetics study indicated that the release process follows the Korsmeyer peppes model. The best efficiency of drug loading for MSN-BS/IBU and MSN-BS/QUE was at 48 h and 25 °C with 250 rpm stirring rate for both IBU and QUE, respectively.

Keywords: Drug delivery; ibuprofen; ionic liquids; mesoporous silica; quercetin

ABSTRAK

Dalam kajian ini, satu siri nanozarah silika mesoliang (MSN) telah berjaya disintesis daripada cecair ion (IL) yang berbeza sebagai templat. Lima jenis IL dan surfaktan dengan rantai sisi alkil dan jenis anion yang berbeza iaitu 1-dodesil-3-metilimidaolium iodida ([C_{12}mim] [I]), 3-dietilamino propanol vanilla (DV), 2-butilamino etanol salsilat (BS), 3-diethilamino propanol salisilat (DS), 1-butil-3-metilimidaolium bis (triflorometilsulfanol) imida ([bmim] [NTf_2]) dan heksadesiltrimetilammonium bromida (CTAB) telah digunakan. Semua MSN yang dihasilkan mempunyai puncak yang luas, hal ini menunjukkan kehadiran silika dalam bentuk amorfus seperti yang diperhatikan oleh XRD, sementara morfologi MSN mendedahkan bahawa penggumpalan zarah adalah disebabkan oleh saiz nanozarah MSN itu sendiri dan saiz liang yang mempunyai susunan selari telah disahkan oleh FESEM dan HRTEM. MSN ini adalah amorfus dan menunjukkan BET isoterma jenis IV dengan gelung histeresis H_2 iaitu jenis isoterma yang sering dikaitkan dengan bahan mesoliang dan luas permukaan tertinggi dicapai adalah 638 m^2/g. Kajian melibatkan penyerapan dan pelepasan ibuprofen dan kuersetin telah dijalankan, yang mana menunjukkan ibuprofen mempunyai penyerapan ubat

yang lebih tinggi berbanding kuersetin disebabkan oleh interaksi yang lebih baik antara MSN dengan molekul ubat. Pelepasan ubat telah dilaksanakan selama 48 jam menunjukkan hanya 33.1% ibuprofen dan 38.4% kuersetin berjaya dilepaskan. Hasil kajian ini menunjukkan bahawa MSN BS merupakan pembawa ubat yang baik untuk ibuprofen. Kajian kinetik berkenaan pelepasan ubat mendedahkan proses pelepasan adalah mematuhi model Korsemeyerpoppes. Kecekapan pemuatan ubat terbaik bagi MSN-BS/IBU dan MSN-BS/QUE adalah pada 48 jam dan 25 °C dengan kadar pengadukan 250 rpm untuk IBU dan QUE.

Kata kunci: Cecair ion; ibuprofen; kuersetin; penghantaran dadah; silika mesoporus

Introduction

Humans have been using drugs to treat illness and diseases for more than 3000 years. The earlier medicinal drugs came from natural sources and existed in the form of herbs, plants, roots, vines, and fungi. Until the 1900s, natural pharmaceuticals were the only solution available to relieve man's pain and suffering. The first synthetic drug, chloral hydrate discovered in 1869 as sedative-hypnotic, is still available in some countries (Costa et al. 2021; Narayan et al. 2018). The post-war period from the 1950s to the 1990s saw major advances in drug development with the introduction of new antibiotics, new analgesics such as acetaminophen and ibuprofen, and completely new classes of pharmaceuticals such as oral contraceptives, ßig-blockers, ACE inhibitors, benzodiazepines, and a wide range of novel anti-cancer medicines (Xie et al. 2016). Since then, each year sees a couple of dozen new drugs licensed for use, but at present, there are tens of thousands of candidate drugs that fell by the wayside.

The research and development journey of those new drugs till its release to the market have taken around 12 years and cost around £1.15 billion (Sriamornsak et al. 2010). However, new approaches in pharmaceutical industries have resulted in more complex drug molecules in the quest to achieve higher affinity to their targets. These highly active drugs can also suffer from poor water solubility. Hence, poorly water-soluble drugs became a big challenge in drug formulation. This problem is increasing, as currently about 40% of the marketed drugs and 90% of drug candidates are classified as poorly water soluble (Maleki et al. 2017). Drug molecule with lack of specificity and solubility lead patients to take high doses of drug to achieve sufficient therapeutic effects. This is a leading cause of adverse drug reactions, particularly for drugs with narrow therapeutic. Various approaches exist to enhance the poor water solubility.

Several different approaches have been designed and utilized to overcome the low solubility of active pharmaceutical ingredients which is an increasing problem in pharmaceutical industries. Thus, many studies investigated different forms of drug delivery carriers. One of the most promising approaches in drug delivery vehicles is mesoporous silica nanoparticle (MSN) as a perfect candidate for this approach. Loading of drugs onto MSN have been considered as a possible strategy to overcome this problem. Mesoporous silica nanoparticles have a number of unique features, such as high surface area, large pore volume and low toxicity (Bharti et al. 2015). The surface area and pore size of the mesoporous materials can be attuned using different types of templates as well as by changing reaction parameters (Vadia & Rajput 2011). As a promising drug carrier, the diameter of MSN can be modified to specifically load either hydrophobic or hydrophilic drugs. The silica surface contains high density of active Si-OH which help targets drug moiety. Due to strong Si-O bond, silica-based mesoporous nanoparticles are more stable to external responses such as degradation (Bharti et al. 2015). Previously, the comparison of non-steroidal anti-inflammatory drug (NSAID) naproxen uptake and release from MCM-41 and SBA-15 matrices was studied by Halamova and Zelenak (2012). In their work, the amount of adsorbed naproxen for the silica SBA-15 was higher compared to MCM-41 due to the two-fold larger pores. However, slightly larger released amount of naproxen (95%) from MCM-41 was observed compared to that of SBA-15 (90%). As reported, this was due to the differences in size of pore and number of pores on the external surface of both materials. The small pores restricted the formation of organized structure inside MCM-41 that led to a lower degree of assembly and high drug disorder in MCM-41. Besides, more mesoporous entrances present on the external surface gave larger possibility for the fluid to penetrate inside channels, dissolving the drug and releasing it into the solution. In other study, Gao et al. (2012) demonstrated three kinds of mesoporous materials bimodal mesoporous silica (BMMs) with short random mesoporous channels. The MCM-41 and SBA-15 were synthesized and modified with NN-

TES to investigate the influence of different structured channels on the controlled ibuprofen delivery. It was found that rate of drug release from 2D MCM-41 was gradually reduced and took about 30 h to release most of ibuprofen. Thus, it would be in more of controlled released when compared with BMMs and SBA-15. Based on Wang et al. (2013), MCM-48 appeared to be a more promising candidate as a solid dispersion carrier offering a high and rapid release, while MCM-41 is more suitable as a drug carrier providing sustained drug release system.

The use of surfactant-template method to synthesize MSN was initially founded by a group of scientists at Exxon Mobil in 1992 (Slowing et al. 2010). The most frequently used template is ionic surfactant. The variation in sizes and shapes of templates leads to formation of mesoporous materials with different pore sizes. Recently, IL is getting attention in many areas of chemistry and industry due to their superior properties. Thus, the great diversity of IL led to mesoporous materials with novel structure and properties. It is notable that the core components of ILs are similar to the ionic surfactant used in the synthesis of MSN, hence ILs are potentially good alternative for template in MSN synthesis. They are ideal solvents for chemical synthesis due to their significant characteristics such as tuneable solvating properties, high thermal stability, very low vapour pressure and nonflammability. These will help to minimize pollutions compare to organic solvents. ILs interact with silicates via electrostatic attraction to form mesopores structures. As previously reported, Li et al. (2008) investigated the effect of amphiphilic room temperature ionic liquid (RTILs) using different alkyl chain lengths. It was discovered that longer alkyl chain lengths of IL tend to form MSN with bigger pore size. This has been related with an additional π-π stacking between the imidazolium ring and long alkyl chain on the cation of IL, which led to the enlargement of pores in MSN. Likewise, Zhang et al. (2009), examined the effects of several anions ($[BF_4]^-$, $[NTf_2]^-$, $[CF_3SO_3]^-$) and cations of IL of MSN formation. It was shown that the alkyl chain length on imidazolium cation and IL concentration in the reaction system significantly impacted the pore structure and thermal stability of the silica gel materials. Mesoporous silicas with 1-alkyl-3-methylimidazolium tetrafluoroborate as the template produced large pore sizes, but yielded lower surface area. This was due to the strength of hydrogen bonds between the water molecules and anions, in the order of $[BF_4]^- < [NTf_2]^- < [CF_3SO_3]^-$(Cammarata et al. 2001).

In this work, ionic liquid templated MSN were synthesized to develop the drug delivery. This is due to the similar core structure of ILs with CTAB in which both consist of inorganic or organic anions and bulky organic cations. One of the advantages of ILs is the wide range of cations and anions that can be used to change their physical properties. The used ILs has diverse combination of cations and anions that can help to improve MSN property as carrier. Thus, the varieties of ILs lead to produce mesoporous materials with different shapes and properties. Then, ibuprofen and quercetin were chosen as a drug model. These drugs are currently used in a range of pharmaceutical formulations as analgesic and anti-inflammatory drugs. They can be impregnated into MSN by reacting with the active groups on the mesoporous framework, for instance by hydrogen bond with surface silanol group (Szegedi et al. 2011). Recent studies on ibuprofen and quercetin, delivery by carriers should facilitate extension of this current knowledge in this fields by giving broader view. Therefore, herein we attempt to synthesis and characterize mesoporous materials with different properties, as well as studying its effect towards drugs. Moreover, the environment condition should also be notable.

Materials and Methods

Materials

Tetrakis (2-hydroxyethyl) orthosilicate (THEOS, 90%) was obtained from Gelest. Ionic liquids (ILs) 1-dodecyl-3-methylimidazolium iodide ($[C_{12}mim][I]$, ≥ 95%), 1-butyl-3-methylimidazolium bis(trifluoromethylsulfonyl) imide ([bmim][NTf_2]) and hexadecyltrimethylammonium bromide (CTAB) were purchased from Sigma-Aldrich while 3-diethylamino propanol vanillate (DV), 2-butylamino ethanol salicylate (BS) and 3-diethylamino propanol salicylate (DS) were synthesized on previous work (Ahmad et al. 2020, 2019a). Ibuprofen (≥ 98%), quercetin (≥ 98%), and phosphate buffer saline (PBS) were obtained from Sigma Aldrich. Ethanol (EtOH, 99.7%) was purchased from HmbG Chemicals. All chemicals except distilled water which was prepared were used as received.

Methods

Synthesis of Mesoporous Silica Nanoparticles (MSN)

The synthesis method was based on the work reported by Postnova et al. (2013) with some modifications. 1.0

mL of IL was dissolved in distilled water (70.0 mL) followed by dropwise addition of THEOS (5.0 mL) under continuous stirring at 60 °C for 1 h (Ahmad et al. 2019b; Rameli et al. 2018). Then, the sample was transferred to a hydrothermal vessel and heated for 24 h at 90 °C. The solid product obtained was filtered, washed with ethanol twice and dried at 80 °C for 24 h. Finally, the product was calcined at 550 °C for 4 h. The same procedure was repeated using different ILs. For clarity, the MSN obtained for each IL were denoted as MSN-C12 ([C_{12}mim][I]), MSN-DV (DV), MSN-BS (BS), MSN-C (CTAB), MSN-DS (DS) and MSN-T ([bmim][NTf_2]).

PHYSICO-CHEMICAL CHARACTERIZATION

FTIR analysis was used to study the framework of MSN and MSN after loaded with drug. FTIR spectra of all the samples were recorded at room temperature on Thermo Scientific Nicolet spectrometer. The sample was grounded using a mortar and pestle until it had approximately the same consistency as the KBr powder. Then, M powder was added, mixed thoroughly with the sample, and then pressed at 9000 tons. The FTIR spectra of all samples were obtained over the range of 4000 to 400 cm^{-1} in transmittance mode. The textural properties of the MSN samples were characterized by N_2 physisorption analysis performed on Micromeritics ASAP 2020 setup. N_2 physisorption measurements were conducted using gaseous nitrogen (N_2) as adsorbate at -196 °C, over 0.01 to 1.00 bar relative pressure range. The synthesized samples were degassed at 200 °C for 2 h at ramping speed of 10 °C min^{-1} for 4 h under vacuum to remove all physiosorbed species from the surface of the sorbent in degas port of the apparatus. The surface area was calculated using Multi-Point Brunnauer-Emmet-Teller (BET) method. The pore size distribution and the pore volume were determined from the desorption branches of the isotherms using the BJH-method. The structural properties were characterized by low angle powder X-ray diffraction (XRD) performed on Bruker AXS D8 Advance Diffractometer with Mn filtered Cu-Kα radiations. Most patterns covered the 2θ angle range of 1 to 28°, with 1.0° step and a step time of 3 s. The XRD patterns indicated the form of samples either as crystal or amorphous. The morphology and the mesostructured were characterized by using field emission scanning electron microscopy (FESEM) on a Ziess Supra 55 VPFESEM microscopy (Germany) operated at 7.00 kV and at magnification of 30 KX. In a typical sample analysis by FESEM, a sample in powder form is deposited on an adhesive carbon tape attached with aluminium stud holder. The excess amount of sample was removed by air spray. The aluminium stud was fixed on the sample holder and then was placed into the vacuum chamber for analysis. High resolution transmission electron microscopy (HRTEM) was used to analyze the pore shape and pore arrangement present in all samples using a JEM-2100F(JOEL) instrument. In a typical sample preparation, sample in powder form was dispersed in a small quantity of ethanol and sonicated for 30 min to disperse the sample into fine particles. Subsequently, the solution was left for 30 min to settle down heavy particles at the bottom and thin particles remain suspended in the solution. The sample were deposited on copper grid 300 mesh by dropping the solution onto the grid, normally air-dried at ambient temperature, and then loaded into the microscope chamber for analysis. The sample was then kept in a vacuum. All the analysis was carried out in vacuum.

DRUG LOADING AND RELEASE

The adsorption method was used to load drug molecules into MSN. IBU was dissolved in ethanol to form a solution with 1.0 mg mL^{-1}. Then, IBU solution mixed with 0.05 g of MSN with continuous stirring to achieve adsorption equilibrium. After 24 h stirring, the precipitated powder was separated by centrifuge at 3500 rpm for 10 min and then washed with ethanol three times to remove the drug on the surface of MSN since the residual drug can be recrystallized on the external surface. Finally, MSN loaded with IBU was dried in an oven at 80 °C for 24 h to remove organic solvent entirely. The UV-vis spectroscopy was used to analyse the quantity of IBU loaded by MSN. 1.0 mL of IBU was obtained and diluted to 10 mL after adsorption and then analyzed at a wavelength of 263 nm. The similar procedure was done for all synthesized MSN. The prepared samples were labelled as MSN-BS/IBU, MSN-C/IBU, MSN-C12/IBU, MSN-DV/IBU, MSN-DS/IBU and MSN-T/IBU. The same procedure also applied on QUE for comparison. 0.1 mL of QUE diluted to 10 mL and the amount of QUE loaded in MSN was determined by using UV-Vis spectrophotometer at 367 nm. The prepared samples were labelled as MSN-BS/QUE, MSN-C/QUE, MSN-C12/QUE, MSN-DV/QUE, MSN-DS/QUE, and MSN-T/QUE. The amount of drug loaded was calculated by Equations (1) and (2) based on the calibration curve of the standard solution. Both Equations (1) and (2) were determined by absorbance versus IBU and QUE concentration, respectively, varying from 0 to 1 mg mL^{-1} and the calibration curve was adjusted to the Beer-Lambert law as follows in Equation (1) and (2):

$$A=1.24x+0.1154 \quad (1)$$

$$A=54.06x-0.0214 \quad (2)$$

where A is the absorbance and x is the concentration in mg mL^{-1}. Meanwhile the percentage of drug loading was calculated using Equation (3):

$$\% \text{ of drug loaded} = \frac{\text{weight of drug loaded (mg)}}{\text{weight of MSN (mg)}} \times 100\% \quad (3)$$

Release studies were conducted by soaking 10.0 mg of MSN/IBU and MSN/QUE samples into 10.0 mL of phosphate buffered saline (PBS) with pH value of 7.4 at 37 °C under steady shaking to prevent internal diffusion limiting the delivery rate. 0.1 mL of the samples were withdrawn at different time intervals and replaced with the same volume of fresh media to ensure the volume is constant. The samples were analyzed at 263 nm for IBU and 367 nm for QUE wavelength of UV-vis spectroscopy. The amount of drugs released was calculated based on Equation (4):

$$\% \text{ Cum. drug release} = \frac{\text{Released drug at difinite time (mg)}}{\text{Amount of drug loaded into MSN(mg)}} \times 100\% \quad (4)$$

DRUG RELEASE KINETIC STUDY

There are five types of fitting models which were the zero order, first order, Higuchi, Hixson-Crowell and Korsmeyer-Peppas models were studied and applied in order to determine which mechanism that controls the drug release kinetic process and best fit drug release model (Equations (5) - (9)) (Heikkila et al. 2007):

$$\text{Zero order:} \quad Q_t = Q_o + k_o t \quad (5)$$

$$\text{First order:} \quad \log Q_t = \log Q_o - \left(\frac{k_2 t}{2.303}\right) \quad (6)$$

$$\text{Higuchi:} \quad Qt = k_H t^{1/2} \quad (7)$$

$$\text{Hixson-Crowell:} \quad Q_t{}^{1/3} = Q_o 1/3 + k_{HC} t \quad (8)$$

$$\text{Korsmeyer-Peppas:} \quad Q_t = kt^n \quad (9)$$

where Q_o is the initial amount of drug; Q_t is the cumulative amount of drug release at time t; K_o, K_1, K_H, and K_{HC} are drug release rate constant of the zero order, first order, Higuchi and Hixson-Crowell models; K is a constant that combined both the geometric and structural characteristics of particles or tablets. Based on Korsemeyer- Peppas equation, the value of n is the diffusion exponent that indicates the release of drug transport mechanism. The release component and kinetic constant value was determined by plotting the graph between a log of cumulative % of drug release vs log times in h. Among these models, the one that showed the biggest correlation coefficient (r^2) will be considered as the best match of the release data.

OPTIMIZATION OF DRUG LOADING AND RELEASE

Optimization of reaction condition for drug loading and drug release was carried out by conventional method. The reaction parameters were optimized by varying one parameter at a time approach. Three different parameters namely time, temperature, and stirring rate were applied. First, drug loading study was varied at different time between 4 and 72 h. The temperature was varied ranging from 25 to 50 °C and lastly stirring rate was studied between 100 and 700 rpm. To optimize the drug release, MSN was soaked with PBS solution at different stirring rate from 100 to 500 rpm. The temperature was maintained at 37 °C to imitate the body temperature.

RESULTS AND DISCUSSION

SYNTHESIS AND CHARACTERIZATION OF MSN

A series of ILs used as a template to stabilize the structure of synthesized MSN via hydrothermal method by using THEOS as precursor. The advantages of THEOS are fast hydrolysis in neutral aqueous solution and the reaction also can take place in broad pH region from 2 to 10. The mass of MSN produced ranged from 20 to 50 mg. The hydrolysis and condensation of MSN using THEOS is well reported by Postnova et al. (2013). The formation of MSN can be understood from the classic nucleation theory (CNT) as reported by Carcouët et al. (2014). However, in this current work, the synthesis of MSN did not follow CNT completely as in agreement with Lv et al. (2016) and Mohamed Isa et al. (2019). According to CNT, particle nucleation requires supersaturation of monomers because of the lack of nucleation centers. However, the micelles formed by ILs act as an additional nucleation centre in the synthesis of MSN.

Figure S1 shows the FTIR spectra of all synthesized MSN ranging from 400 to 4000 cm^{-1}. The presence of surface silanol (Si-OH), hydroxyl (-OH) and siliceous framework structure of MSN were seen from the FTIR spectra. It was observed that the FTIR spectra of all MSN showed similar peaks. Typically, MSN exhibits IR peaks at the band attributed to Si-O-Si bending (450.43 to 455.05 cm^{-1}), Si-O-Si symmetric stretching (801.37 to 806.37 cm^{-1}), external Si-OH group (944.09 to 946.54 cm^{-1}), Si-O-Si asymmetric stretching (1054.65 to 1069.88 cm^{-1}), and -OH stretching at 3455 cm^{-1} (Kamarudin et al. 2013; Zaharudin et al. 2020). After calcination, the MSN

still retained its siliceous structure. The FTIR spectra displayed no major changes in the formation of MSN framework. The relative intensity of all Si-O and Si-O-Si vibration modes for calcined MSN became more intense, suggesting the existence of Si-O-Si interaction at the inner surface of MSN after ILs removal.

The XRD pattern for each MSN is shown in Figure 1 ranging from 2θ = 2 to 25°. It was found that no peaks were observed at the small angle region of 2° for all MSN indicating that all MSN produced amorphous materials with parallel pore ordering supported with HRTEM image Figure 2(c). Commonly, MCM-41 exhibit peaks at 2θ of 2.17, 3.74 and 4.35°, respectively, assigned to hexagonal mesopores structure (Ab Wab et al. 2014). The presence of these peaks indicates the presence of long-range crystalline structure. Kamarudin et al. (2013) also reported similar observation with three main peaks at 2θ = 2.2, 3.9 and 4.5°, respectively. However, in this work the amorphous phase was observed at a broad peak around 2θ = 20 to 25°, which agreed with previous work (Ward et al. 2011) which indicated the non- and semi-crystalline silica. The lack of sharp signals in these XRD patterns could be due to the lack of large diffraction domains caused by the small nanoparticle size of MSN. Surprisingly, for MSN-T, the XRD spectrum showed a visible peak at 2θ = 2.3°, while MSN-C12 exhibited a peak signal at 2θ = 6.3° though both displayed low intensities. This can be explained by considering the formation of order pores, but insignificant.

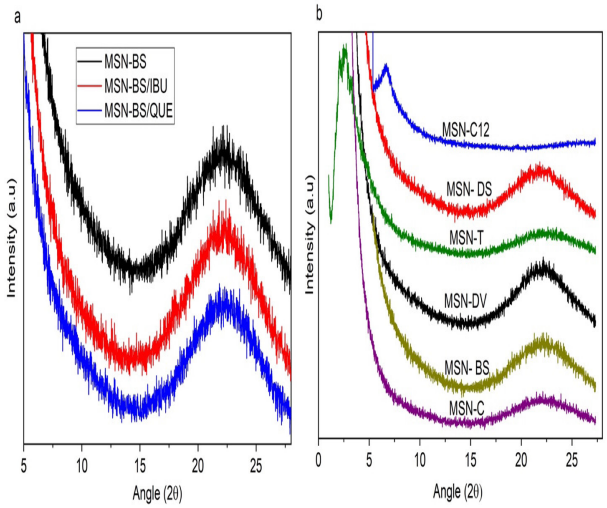

FIGURE 1. XRD pattern of synthesized MSN-templated ionic liquids

The N_2 adsorption-desorption results as shown in Figure S2 illustrates that the synthesized MSN exhibits Type IV isotherm based on the IUPAC classification, which is the characteristic of mesoporous materials with H2 hysteresis loop. There was a slight increase in the initial part of the isotherm which indicates the stage at which monolayer coverage completed and multilayer adsorption started. There was also a steep increase of adsorption process and a sharp desorption branch observed at around P/P_o = 0.8 which formed H2 hysteresis loop. This hysteresis loop associated with mesopores of MSN indicates ink-bottleneck type pores that are not well-defined and irregular, indicating pore blocking inside the channels. This occurrence is usually due to pore constriction during evaporation of the capillary condensate (Cammarata et al. 2001). The desorption was delayed due to the desorption pressure by the opening of smaller pores that may happen by percolation. BET analysis was used to determine the surface area, pore size and pore volume of synthesized MSN as tabulated in Table 1. It was observed that MSN-BS has the highest surface area of 638 m^2/g, with almost a two-fold difference compared to the lowest surface area displayed by MSN-T (357 m^2/g). The surface area of MSN was arranged as followed: MSN-BS > MSN-C > MSN-C12 > MSN-DV > MSN-DS > MSN-T. This trend of MSN surface area might be due to the anion size that can be explained based on the anions' strength of hydrogen bond with water (Kamarudin et al. 2013). This phenomenon can be explained through the basics

of Classic Nucleation Theory (CNT), but in a slightly different way (Mohamed Isa et al. 2019). Generally, MSN were formed via charged-mechanism where the charge interaction occurs between the cationic template (S^+) and silicate oligomers (I^-) to form the S^+I^- assembly.

TABLE 1. Comparison of the surface area, pore volume and pore size of unloaded MSN samples and IBU and QUE-loaded MSN and release

Samples	BET (m^2/g)	Pore volume (cm^3/g)	Pore size (nm)	Drug content (mg/g)	Drug loading (%)	Drug release (%)
MSN-BS	638	0.99	7.47	-	-	-
MSN-BS/IBU	502	0.79	5.51	656.09	65.6	33.1
MSN-BS/QUE	445	0.94	5.31	302.08	30.2	38.4
MSN-C[a]	595	1.11	7.64	-	-	-
MSN-C/IBU	496	0.65	5.65	639.50	64.0	26.4
MSN-C/QUE	480	0.94	7.56	284.06	28.4	35.1
MSN-C12	557	1.09	7.82	-	-	-
MSN-C12/IBU	463	1.04	6.00	535.81	53.6	24.7
MSN-C12/QUE	546	0.83	7.20	266.52	26.6	33.1
MSN-DV	427	0.94	8.71	-	-	-
MSN-DV/IBU	390	0.87	7.66	520.48	52.1	21.4
MSN-DS/QUE	416	0.92	8.64	252.17	25.2	30.34
MSN-DS	375	1.13	11.06	-	-	-
MSN-DS/IBU	369	1.09	8.88	498.40	49.9	18.7
MSN-DS/QUE	328	0.93	10.06	248.02	24.8	27.4
MSN-T	357	0.93	10.23	-	-	-
MSN-T/IBU	270	0.86	8.23	451.47	45.1	15.9
MSN-T/QUE	342	0.64	7.21	239.59	24.0	24.7

This study discovered the size of anions contributes to the production of higher surface area of MSN similar to Cammarata et al. (2001). They found that the strength of anion's hydrogen bond increased in the order of $BF_4^- < ClO_4^- < NO_3^- < CF_3COO^- < Br$. In this study, it can be deduced that the affinity of IL anions towards water molecules in the solution was higher forming hydrogen bonds. This situation leads to the decrease of anion electrostatic attraction towards cation. The trend in this study can be explained by the higher strength of intermolecular hydrogen bond. The poor interaction between IL anion and cation led to a stronger interaction between the cation micelle with a positive charge and silicate oligomers that are negatively charged. This resulted in the building of silica-template composite, which led to nanoparticles being formed. This was due to the strength of hydrogen interactions between these ILs anion and water molecules. It was suggested that anion ILs used in this work contribute and affect the production of MSN. Likewise, the mesoporous silicas with 1-alkyl-3-methylimidazolium tetrafluoroborate have been found by Zhang et al. (2009) through the large pore sizes formed by the template, although they have a lower surface area. It was found that MSN-DS has the largest pore size and pore volume compared to the other MSN. This might due to the particle size and loosely connected mesoporous silica. The bulkier size molecule also caused difficulty in the formation of micelle (Hong et al. 2009).

Figure 2(a) and Figure 2(b) illustrates the images of MSN-BS and MSN T representing the other synthesized MSN due to the behavior of morphology similarity observed from XRD. It can be seen that for MSN-BS, the surface was smooth and homogenous while MSN-T was found to be rough with big agglomerate. This can be explained by the effect of template used. This morphology was consistent with N_2 sorption obtained where the surface area of MSN-BS was high. The porous surface of MSN-T was observed as agglomerate particle with no definite shape of particle observed due to the attractive force between silanol group. The particles colloid and suspension were unstable, which led to agglomeration. The agglomeration of samples always preferred over nanoparticles since it reduces surface area and saturates the bonding (Beltrán-Osuna et al. 2017). Based on the FESEM morphology, MSN-T have a high degree of roughness that was mutual with the presence of $Si(OH)_2$ groups. The result obtained was quite similar with previous work carried out by Kamarudin et al. (2013) where they found the formation of agglomerated spherical MSN in their work.

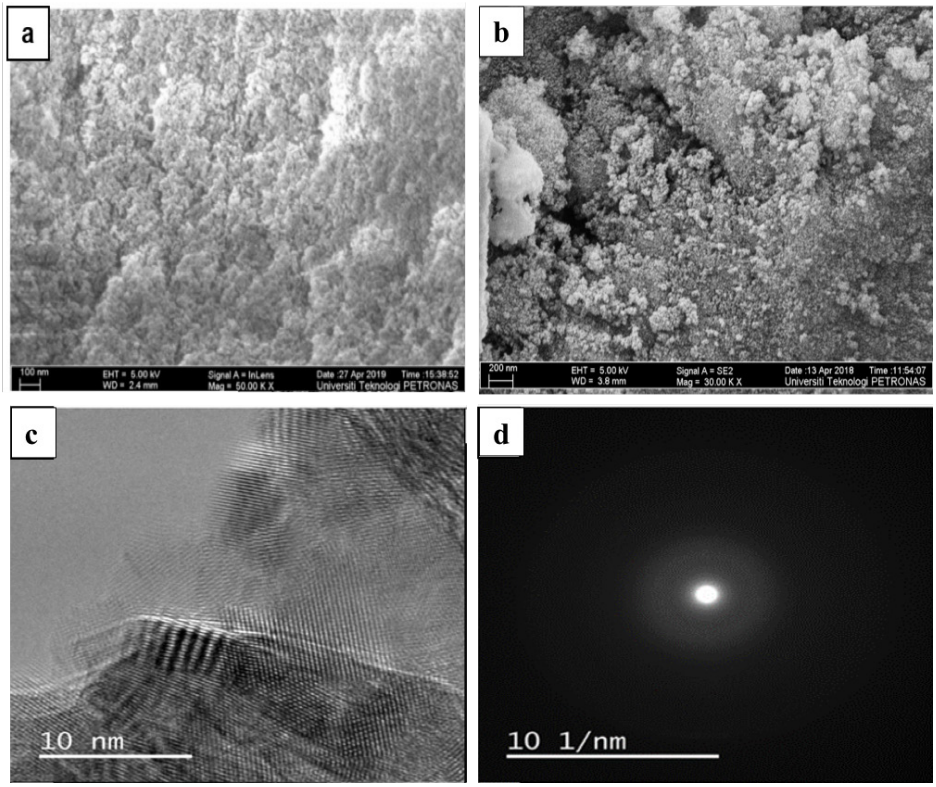

FIGURE 2. Images of (a) FESEM of MSN-BS, (b) FESEM of MSN-T, (c) HRTEM, and (d) SAED of MSN-BS

HRTEM analysis provides information about the pore structure and pore arrangement present in MSN. MSN-BS was chosen to represent the MSN samples due to similar patterns morphology observed. Figure 2(c) showed a large number of parallel pore arrangement of MSN-BS. This formation was suggested to be driven by the interface between the silica/ILs surfactant stage being evenly attractive toward polar and non-polar species. The HRTEM image of MSN showed similar behaviour to that of MCM-41 in Szegedi et al. (2011) work. They found that MCM-41 has parallel straight channel crossing the entire particles. Figure 2(d) also showed selected area electron diffraction (SAED) of MSN to determine the crystalline of the sample. Additionally, SAED analysis was performed on individual particle ensembles showed a diffused spot typically for amorphous materials, reiterating the amorphous nature of silica.

DRUG LOADING AND DRUG RELEASE

The estimated amounts of drugs loaded into MSN after immersion of 24 h ranged from 451.47 to 656.09 mg/g (drug/carrier) for IBU, while QUE was in the range of 239.59 to 302.08 mg/g (drug/carrier), as tabulated in

Table 1. The incorporation of IBU and QUE into MSN was significantly affected by the surface area, pore size, and pore volume of synthesized MSN. As expected, the MSN surface area, pore size, and pore volume reduced with the loading of drugs. IBU and QUE has molecular weight of 206.29 and 302.12 g/mol and the molecular structure of both drugs were showed on Figure S3. Both of drugs are compatible with MSN pores, resulting in more IBU adsorption into MSN. From the results obtained, it can be concluded that MSN preferred to accommodate IBU as compared to QUE. This can be explained by the difference in size of drug molecules that can fit into the mesopores framework. Therefore, the ability of IBU to incorporate into MSN mesopores was better than QUE. Among the synthesized MSN, MSN-BS with the highest surface area adsorbed 65.6 and 30.2% of IBU and QUE, respectively. Surface area is a crucial influence that determine the amount of retained drug molecules adsorbed, generally due to the chemical and physical adsorption property of Si-OH groups in drug loading method. The analysis of Table 1 showed that the surface area and pore volume were decreased as the drugs were loaded. The high surface area of MSN-BS means more Si-OH groups are available to provide more active sites, thus increasing drug loading capacity for IBU and QUE. During the uptake, IBU and QUE molecules can be adsorbed onto the surface of MSN via impregnation process. The hydrogen bond interaction of IBU and QUE molecules with silanol group existing in the pore walls of MSN controls the adsorption of drug molecules to the surface and inside the channels.

The pore size is crucial for drug loading because it acts as molecule sieves and they can determine how large drug molecules can be loaded into carrier. After immersing MSN into IBU and QUE solution, MSN-BS with small pore size loaded high drugs compared to MSN-T with large pore size. As presented in Table 1 it can be deduced that as the pore size increases, the drug uptake decreases. This can be explained due to the close packing of IBU and QUE molecules along the pore wall causing the IBU and QUE to compete among themselves to bind with Si-OH due to steric hindrance of drugs. Thus, this could be a reason that IBU and QUE were not fully bind with silanol group of MSN.

In order to study the performance of MSN in a drug delivery application, *in vitro* IBU and QUE release using a phosphate buffer silane (PBS) and ethanol solution was carried out. Results showed that a fast drug release occurred in the initial period while the maximum release of IBU and QUE was obtained after 48 h for all MSN Figure 3. MSN-BS released the highest IBU and QUE among the synthesized MSN which were 33.1 and 38.4%, respectively, while MSN-T released the lowest drug with 15.9 and 24.7% as tabulated in Table 1. This may be due to the weak interaction between the hydroxyl group of IBU and the silanol group of MSN. The drug release of IBU and QUE increased as the pore size decreased. MSN-BS with the smaller pores released the highest drugs compared to MSN-T. It can be deduced that the degree of drugs crystallinity was lower in the smaller pore which should increase the release of drug. The larger pore size of MSN samples has been reported to boost recrystallization (Mohamed Isa et al. 2018; Quevedo et al. 2018). The blockage from crystalized drugs formed slowed down the release of drug. Moreover, the trend of drug release of MSN for both drugs were similar. However, the drug release of MSN loaded with IBU was lower compared to MSN loaded with QUE. This is due to the strong interaction of IBU with silanol groups of MSN. The steric hindrance among the QUE molecules also helped in the release of QUE.

During the release process, the solvent entered IBU and QUE matrix phase through the pores. The beginning

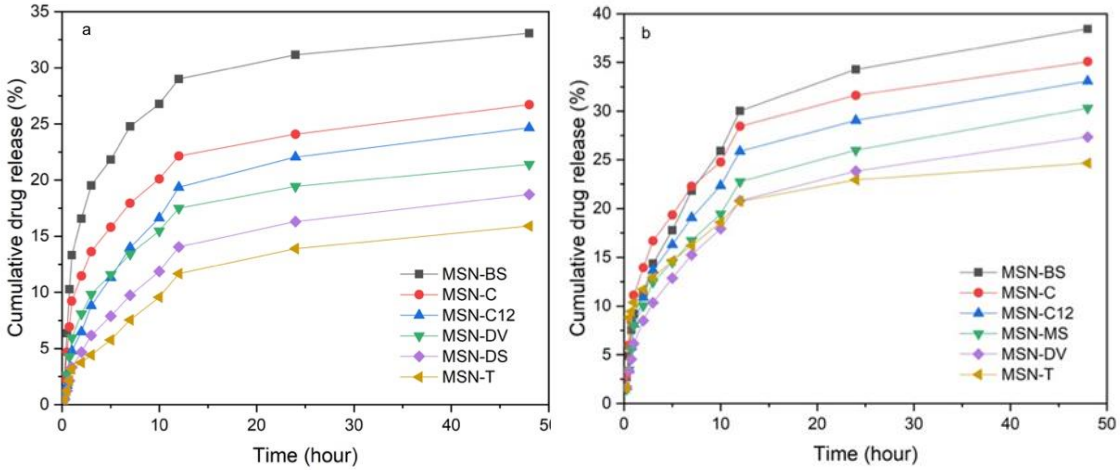

FIGURE 3. Drug release profile for synthesized MSN with (a) IBU, and (b) QUE

of 8 h, drug delivery was faster in the initial testing time and after that the drug release from samples gradually slowed down. The initial burst was attributed to the immediate dissolution of IBU and QUE located on the external surface and near the surface of MSN. Moreover, the MSN/IBU and MSN/QUE showed delayed release described by the corrugated porous framework with porous windows linking the larger main pores called bottle-neck effect (Maleki et al. 2017). This behavior indicates that some drugs molecules were adsorbed close to the initial part of the channels in the MSN on the outer surface and were quickly released in the beginning of the release process. As in this second step after 8 h, IBU and QUE inside the porous channels were released more slowly. This was due to the interaction of the drug molecules with silanol group, thus requiring more time for the molecules to leave the silica channel. Hence, the pore type expected based on the isotherm type may had affected the release of IBU. In addition, the multilayer physical adsorption during drug loading was unstable and led to low utilization of mesoporous channels. Thus, the weak interaction of the abundant drugs molecules with silanol groups led to the release of drug (Maleki et al. 2017; Xu et al. 2010).

FTIR analysis of drug loaded and released from MSN samples was performed to detect any structural changes on the synthesized MSN. Figure S4 shows the FTIR spectra of MSN with loaded drugs, IBU and QUE. The FTIR peaks of unloaded MSN were quite similar with drug-loaded MSN. The characteristics of IBU and QUE peaks were not obviously established, suggesting the existence of primary feature bands of MSN component. This may be due to the small amount of IBU and QUE loaded into MSN. It was seen that MSN pores were not

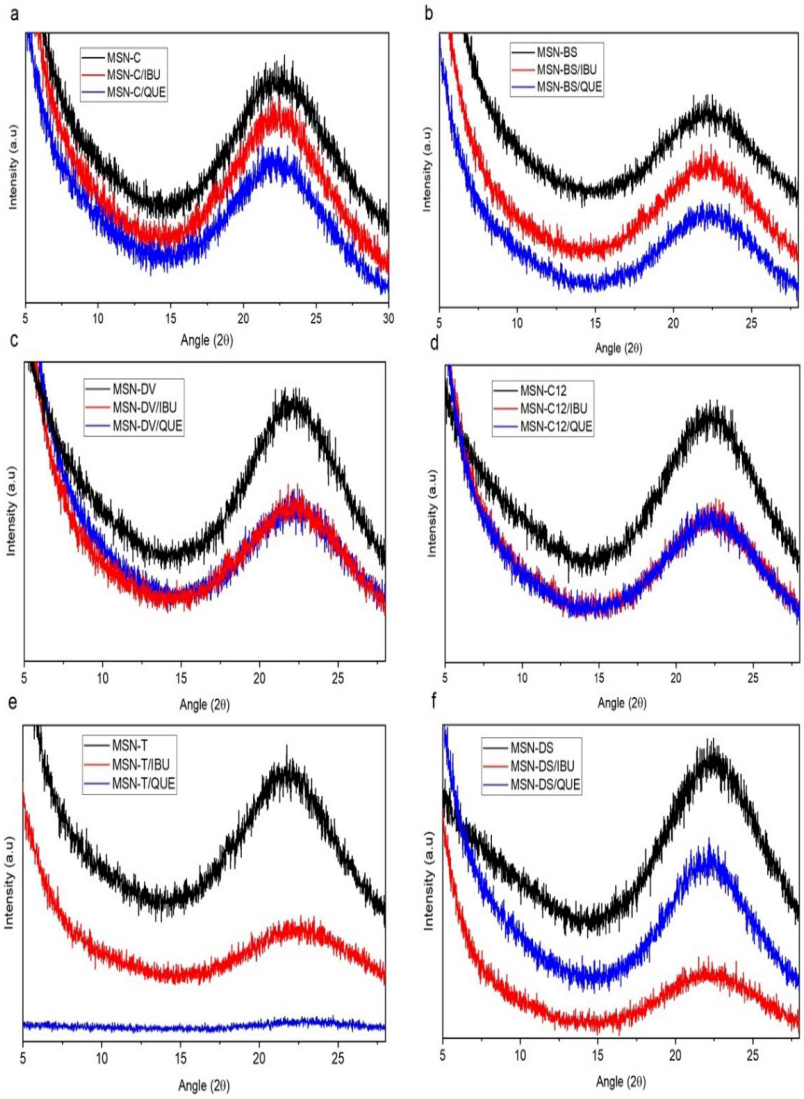

FIGURE 4. XRD of synthesized MSN loaded with IBU and QUE: (a) MSN-C, (b) MSN-BS, (c) MSN-DV, (d) MSN-C12, (e) MSN-T, and (f) MSN-DS

damaged by the inclusion of IBU and QUE. XRD analysis was performed to observe the effect of drugs on the MSN crystallinity. The XRD patterns of the unloaded MSN and drug-loaded MSN were shown in Figure 4. It showed that the broad amorphous phase of silica was present between 2θ = 15 to 28° for all unloaded MSN and drug-loaded MSN. In general, the XRD pattern of MSN displayed amorphous behavior even after loaded with drugs. Once the drug was loaded into MSN, the peak intensity reduced owing to the filling of empty spaces within the pores of MSN.

N_2 sorption isotherm was used to determine the loading efficiency of IBU and QUE in mesopores of synthesized MSN. The N_2 sorption isotherm of MSN were shown in Figure S5. The figure shows that the isotherm for unloaded MSN and drug-loaded MSN were Type IV isotherm with H2 hysteresis loop, indicating the mesostructure of MSN was not disturbed after incorporation of drugs. However, the intensity of N_2 sorption isotherm decreased compared to bare MSN after IBU and QUE was loaded into the MSN. This trend can be explained due to the filling of drugs into MSN pores. It was also observed that MSN loaded with IBU has lower intensity compared to MSN loaded QUE and can be explained due the size of IBU. IBU has a smaller size compared to QUE, allowing IBU to occupy more pore surface area. This finding was similar with Kamaruddin et al. (2013), where they found that the isotherm

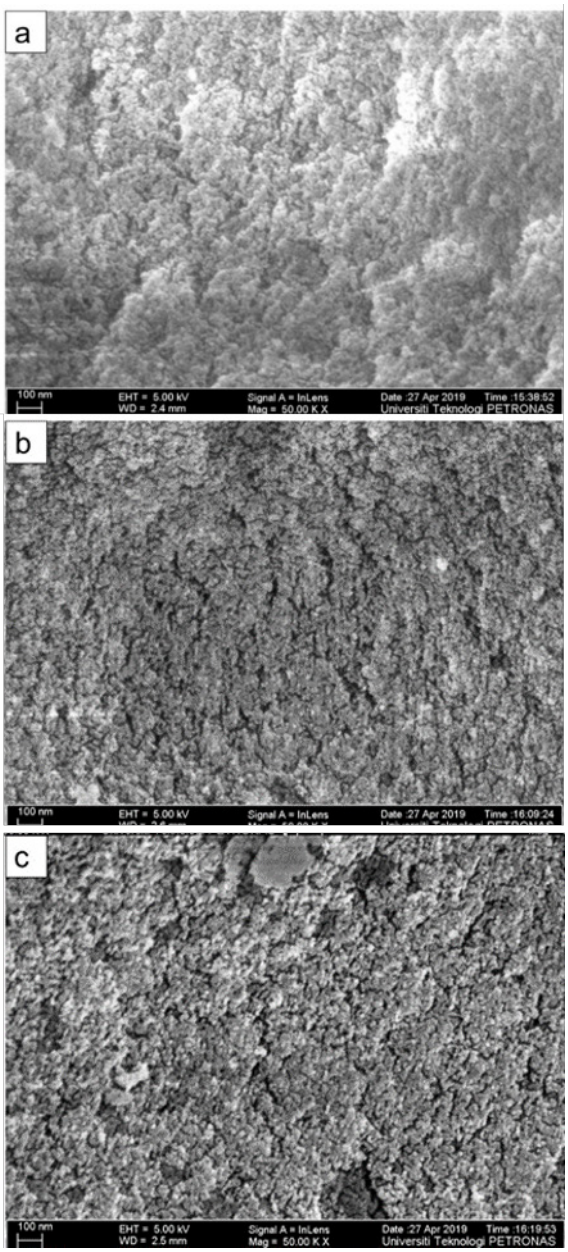

FIGURE 5. FESEM images of (a) bare MSN-BS, (b) MSN-BS/IBU, and (c) MSN-BS/QUE

before and after drug uptake were similar. The stages of N_2 adsorption phase for unloaded MSN and drug-loaded MSN remained the same. The steep increase of adsorption indicated the hysteresis loop (H2) which is the characteristic of capillary condensation of the nitrogen that occurred inside the mesopores. The adsorption of IBU and QUE molecules onto the surface and inside of MSN was controlled by hydrogen bond interaction between drugs molecules and silanol group present in the pore walls and the adsorption mechanisms depend on the pore size and the size of drug. When the pore size is much larger than the drug molecules, a close packing of drug molecules takes place causing the pore size to reduce, but it does not fully occupy the space available for N_2 adsorption (Sabbagh & Muhamad 2017).

FESEM morphology was obtained to determine the effect of drugs (IBU and QUE) on the surface of MSN after the drug uptake. Figure 5 presents FESEM micrographs of MSN-BS, MSN-BS/IBU and MSN-BS/QUE. In this result, MSN-BS, MSN-BS/IBU and MSN-BS/QUE represent the synthesized MSN and MSN with loaded drugs. From the FESEM images, MSN-BS showed homogenous and smooth surface. However, as IBU and QUE were loaded into MSN-BS, the surface of MSN-BS particles resulted in more aggregation and rougher particles as the mesopores were filled with drugs molecules attached on it and spread out on the external surface. The morphology of MSN-IBU and MSN-QUE more intense due to its distribution in the carrier.

Analysis of the HRTEM patterns of MSN-BS, MSN-BS/IBU and MSN-BS/QUE are shown in Figure 6. Similarly, as FESEM results, MSN-BS was chosen to represent all MSN since it was the best in loading drugs in this work. The HRTEM images of MSN-BS/IBU and MSN-

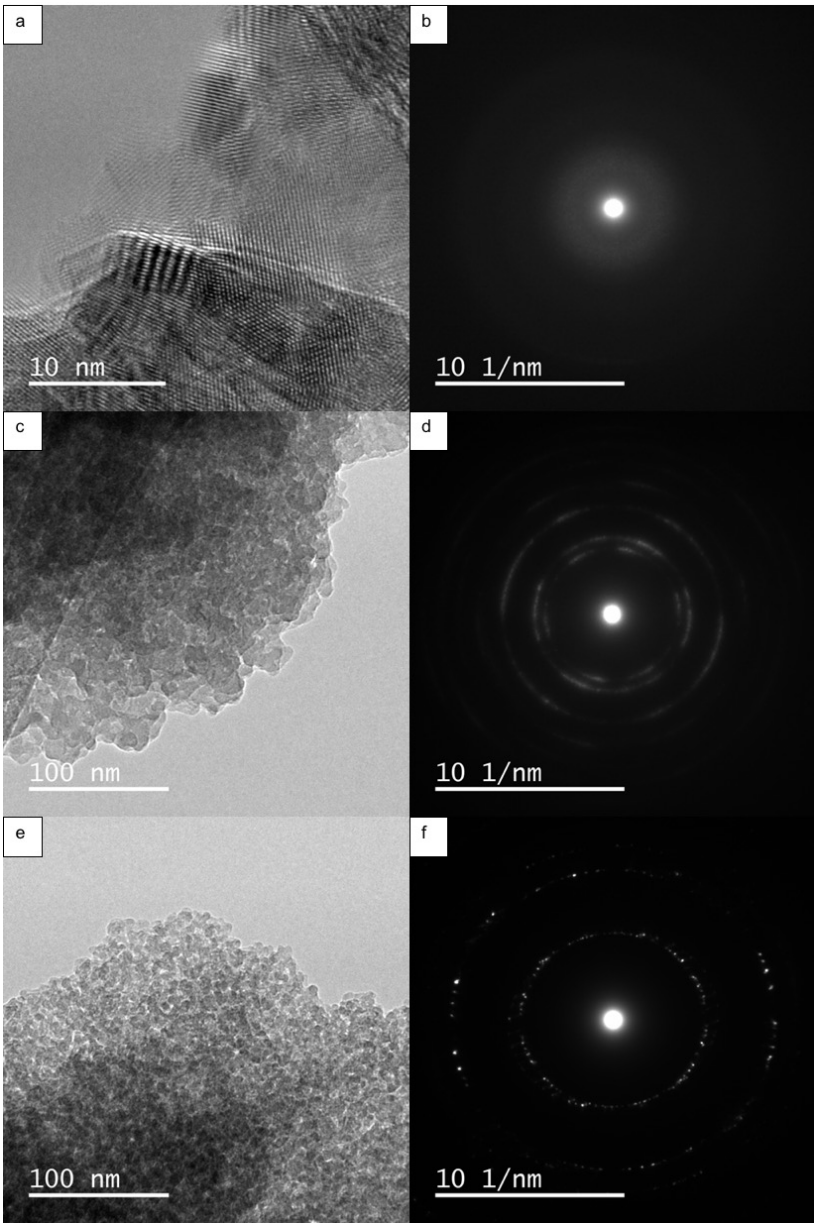

FIGURE 6. HRTEM images of (a) bare MSN-BS, (c) MSN-BS/IBU, and (e) MSN-BS/QUE, and SAED of (b) bare MSN-BS, (d) MSN-BS/IBU, and (f) MSN-BS/QUE

BS/QUE clearly showed the ordered pore arrangement was well disturbed. It can be deduced that IBU and QUE were filling into mesopores of MSN and drugs did affect structural integrity of MSN-BS. Apart from that, SAED results were also obtained to compare the changes of MSN-BS sample before and after the drugs was loaded. Figure 6(d) and Figure 6(f) shows a ring like pattern, which indicated the amorphous with poorly crystalline state of MSN-BS/IBU and MSN-BS/QUE (Saptiama et al. 2018). This pattern can be explained because of the present of IBU and QUE inside MSN-BS during the drug loading. The crystallization may occur due to the rapid diffusion of drugs based on the drugs size that can passed the pore of MSN. It was observed that MSN-BS/IBU had significant ring pattern compared to MSN-BS/QUE due to high loading of IBU compared to QUE. This can be explained by the higher loading of IBU compared to QUE. It was consistent with the calculated result where IBU was loaded two times higher (about 60%) compared to QUE (30%).

DRUG RELEASES KINETIC STUDIES

In order to study the mechanism and kinetic of drug release process, the experimental data were fitted into zero order, first order, Higuchi, Hixson- Crowell and Korsmeyer-Peppas equations. The linear plots of release kinetics were attained for ibuprofen and quercetin released from all of the synthesized MSN to determine the best fit of model. The parameters of all released kinetic models of both drugs were presented in Tables 2 and 3, respectively. It was discovered that the release of both drugs from all synthesized MSN follows and fitted with the Korsmeyer-Peppas's kinetic model which suggests that the drugs were released.

Korsmeyer-Peppas equation can explained the mechanism of drug release from MSN. The value of release exponent, *n* also was determined from the slope gradient line. The calculated value of *n* indicates that the release mechanism follows the non-Fickian diffusion. This mechanism explains that the initial release of drugs might occur due to discharging of drugs from MSNs pore entrances before dissolve slowly into the medium from mesochannel and finally followed by dissociation of hydrogen bond from the drugs with MSN (Heikkila et al. 2007; Sabbagh & Muhamad 2017).

TABLE 2. Models fitting for ibuprofen release kinetics

	Zero order	First order	Higuchi	Hixson-Crowell	Korsmeyer-Peppas
	R^2	R^2	R^2	R^2	R^2
MSN-BS	0.8639	0.8822	0.9526	0.8760	0.9875
MSN-DV	0.9203	0.9275	0.9582	0.9247	0.9882
MSN-DS	0.9556	0.9590	0.9403	0.9576	0.9700
MSN-T	0.8579	0.8612	0.9318	0.8592	0.9703
MSN-C12	0.9563	0.9606	0.9397	0.9589	0.9617
MSN-C	0.8752	0.8877	0.9682	0.8831	0.9879

TABLE 3. Models fitting for quercetin release kinetics

	Zero order	First order	Higuchi	Hixson-Crowell	Korsmeyer-Peppas
	R^2	R^2	R^2	R^2	R^2
MSN-BS	0.8858	0.8993	0.9759	0.8943	0.9833
MSN-DV	0.9041	0.9136	0.9546	0.9101	0.9810
MSN-DS	0.6370	0.651	0.8344	0.6459	0.8348
MSN-T	0.9254	0.9333	0.9790	0.9301	0.9862
MSN-C12	0.9286	0.9382	0.9610	0.9347	0.9791
MSN-C	0.8800	0.8957	0.9729	0.8902	0.9911

PROCESS OPTIMIZATION DRUG LOADING

Ibuprofen (IBU) and quercetin (QUE) were loaded into MSN-BS which has the highest surface area among the MSN synthesized. The loading reaction was performed at different times, temperatures, and stirring rates to achieve the highest amount of drug loaded. Figure 7 shows the loading of drugs against time. The percentage of drug loading for IBU as shown in Figure 7(a) gave the highest drug loading at 48 h with 66.1%. It showed a rapid increase of drug loading in the initial 24 h, followed by a gradual increment from 24 to 48 h and decreased after 48 h. This may be related to the potential intermolecular interaction between MSN and the solvent. The possibility of the hydrogen bonding between ethanol and the pore surface may compete with the drug adsorption as the time extended (Mccarthy et al. 2016). The hydrogen bonding of ethanol with drug can also occur causing the recrystallization of IBU slowing down the uptake of drug (Irvine et al. 2018; Vallet-Regí et al. 2018).

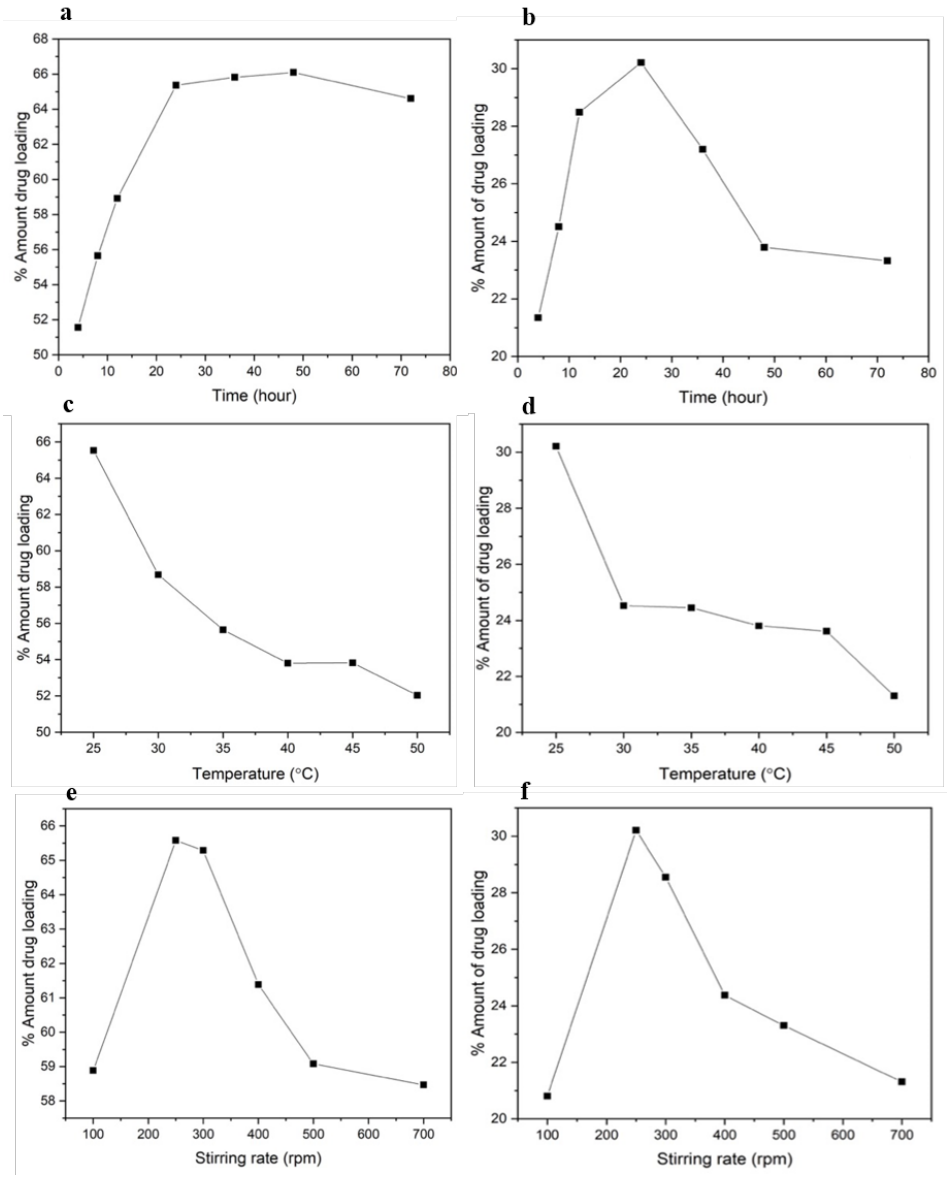

FIGURE 7. Drug loading percentage into MSN-BS at different times, different temperatures, and different stirring rates for (a), (c), (e) for IBU, and (b), (d), (f) for QUE

Based on graph trend obtained for drug loading of QUE in Figure 7(b), the highest drug loading obtained was 30.2% within 24 h. After the maximum point, the percentage of QUE loading was found to decrease rapidly within 72 h. It was apparent that this trend was quite similar with IBU. The optimum uptake time for both drugs was the same at 24 h. However, MSN can load IBU until 48 h due to the smaller molecular weight of IBU. The percentage of drug loading in MSN for IBU and QUE continuously decreased, which can be explained by the degradation process due to nucleophilic attack by hydroxide of ethanol into SiO_2 network. This reaction caused hydrolytic breakdown of the siloxane (Si-O-Si) group and leaching of orthosilicic acid ($Si(OH)_4$) (Li & Yang 2015). Thus, high surface area causes the silica matrix leach due to the great contact with physiological medium at long period.

Figure 7(c) and Figure 7(d) shows the effect of varying temperatures on the percentage of drug loading. The highest amount of drug loaded was achieved for MSN-BS/IBU (65.5%), while MSN-BS/QUE was only 30.2% at a temperature of 25 °C. The percentage of drug loading decreased after 25 °C for both drugs. As shown in Figure 7(c), from 25 to 40 °C, the percentage of drug loading rapidly decreased, followed by a slight decreased from 40 to 50 °C for IBU loading. This was caused due to the heating process, resulting in a reduction of hydrogen bonding strength. As known, IBU has only an -OH group. As temperature increases, the hydrogen bonding can be easily weakened. However, in Figure 7(d) for QUE loading, a significant decrease was observed from 25 to 30 °C. Then, a continuously decrease of drug loading was observed from 30 to 45 °C, followed by a rapid decrease of QUE loading at 45 to 50 °C. Increasing the temperature would increase the kinetic energy of molecules and would thus lead to the weakening the intermolecular hydrogen bonds between these drugs and synthesized MSN. Thus, the mass transfer of IBU and QUE molecules into the channels became slow (Hashemikia et al. 2015). When the temperature increased, the bond became weak causing the drugs to be loosely held on the surface of MSN and lost during washing stage (Li et al. 2016).

Figure 7(e) and Figure 7(f) presents the effect of different stirring rate in the range of 100 to 700 rpm on the percentage of drug loading. The graph shows that the highest loading of IBU was 65.6% and QUE was 30.2% at 250 rpm of stirring speed. The drug loading needed an optimum process requiring diffusion of the IBU and QUE molecules from ethanol solution onto the mesoporous silica surface. This gave the drug molecules some time to be rearranged and deposited in the mesopores accordingly. As can be seen, the percentage of drug loaded into the MSN increased with increasing stirring rate from 100 to 250 rpm. However, after 300 rpm of stirring effect, a rapid decrease of the amount of drug loading for both drugs were observed. Similar trends have been observed in stirring rate curve for IBU and QUE loading. At a higher speed exceeding the optimum rate, drug molecules entered the pores rapidly. Then, it is possible that drug molecules were adsorbed into the surface quickly and could block the mesopores preventing the access to further drug binding sites located deeper in the porous material and causing the crystallization of drug (Irvine et al. 2018; Li et al. 2016). The crystallization might be due to the drugs and ethanol interaction that enhanced crystal growth with the help of high speed of stir.

Conclusion

This study discovered an approach to synthesize silica mesopores using ILs as a template for drug loading and release from MSN. MSN have been successfully synthesized by hydrothermal method with THEOS as precursor and ILs as a template. The prepared MSN were characterized by various analytical techniques to explore their physicochemical properties. The results showed that the physiochemical properties of the prepares MSN varied depending on the cation alkyl chain length and hydrogen bond strength of anion used. MSN-BS has the highest surface area of 638 m^2/g with 7.47 nm pore size. Furthermore, this study has shown how textural properties in MSN results in accessible materials, facilitating the drug load inside the MSN. Among the MSN tested, MSN-BS was the best MSN that can load the highest rate of 65.6% IBU and 30.2% QUE, respectively. The efficiency of loading was correlated to the surface area and pore size of the MSN. The high surface area means more Si-OH groups that provide more active sites, thus increasing drug loading amount. The drug release of MSN-BS/IBU and MSN-BS/QUE has the highest release cumulative amount of drug release, which was 33.1 and 38.4%, respectively. The best loading efficiency was achieved in 48 h at 25 °C with stirring rate of 250 rpm for IBU and QUE. Drugs release kinetics study indicated that the release process follows the Korsmeyer peppes model. These MSN have the promising textural properties for providing a slow release of drugs from mesoporous materials.

ACKNOWLEDGEMENTS

This research was funded by the STIRF Research Grant 0153AA-F21. The authors are grateful to the Universiti Teknologi PETRONAS for the UTP Graduate Assistantship (GA) scheme support for Najihah Rameli.

REFERENCES

Ab Wab, H.A., Abdul Razak, K. & Zakaria, N.D. 2014. Properties of amorphous silica nanoparticles colloid drug delivery system synthesized using the micelle formation method. *Journal of Nanoparticle Research* 16(2): 2256.

Ahmad, N.A., Jumbri, K., Ramli, A., Ahmad, H., Rahman, M.B.A. & Wahab, R.A. 2020. Design and molecular modelling of phenolic-based protic ionic liquids. *Journal of Molecular Liquids* 308: 113062.

Ahmad, H., Zaharudin, N.S., Majid, N.N.A., Jumbri, K. & Rahman, M.B.A. 2019a. Synthesis and characterization of new choline-based ionic liquids and their antimicrobial properties. *Journal of Advanced Research in Fluid Mechanics and Thermal Sciences* 54(2): 124-132.

Ahmad, N.A., Jumbri, K., Ramli, A., Ghani, N. & Ahmad, H. 2019b. Salicylate-based protic ionic liquids as a potential antioxidant. *Malaysian Journal of Analytical Sciences* 23(3): 383-389.

Beltrán-Osuna, Á.A., Gómez Ribelles, J.L. & Perilla, J.E. 2017. A study of some fundamental physicochemical variables on the morphology of mesoporous silica nanoparticles MCM-41 type. *Journal of Nanoparticle Research* 19(12): 381.

Bharti, C., Nagaich, U., Pal, A.K. & Gulati, N. 2015. Mesoporous silica nanoparticles in target drug delivery system: A review. *International Journal of Pharmaceutical Investigation* 5(3): 124-133.

Cammarata, L., Kazarian, S.G., Salter, P.A. & Welton, T. 2001. Molecular states of water in room temperature ionic liquids. *Physical Chemistry Chemical Physics* 3(23): 5192-5200.

Carcouët, C.C.M.C., Van De Put, M.W.P., Mezari, B., Magusin, P.C.M.M., Laven, J., Bomans, P.H.H., Friedrich, H., Esteves, A.C.C., Sommerdijk, N.A.J.M., Van Benthem, R.A.T.M. & De With, G. 2014. Nucleation and growth of monodisperse silica nanoparticles. *Nano Letters* 14(3): 1433-1438.

Costa, J.A.S., De Jesus, R.A., Santos, D.O., Neris, J.B., Figueiredo, R.T. & Paranhos, C.M. 2021. Synthesis, functionalization, and environmental application of silica-based mesoporous materials of the M41S and SBA-n families: A review. *Journal of Environmental Chemical Engineering* 9(3): 105259.

Gao, L., Sun, J., Zhang, L., Wang, J. & Ren, B. 2012. Influence of different structured channels of mesoporous silicate on the controlled ibuprofen delivery. *Materials Chemistry Physics* 135: 786-797.

Halamova, D. & Zelenak, V. 2012. NSAID naproxen in mesoporous matrix MCM-41: Drug uptake and release properties. *Journal of Inclusion Phenomena and Macrocyclic Chemistry* 72: 15-23.

Hashemikia, S., Hemmatinejad, N., Ahmadi, E. & Montazer, M. 2015. Optimization of tetracycline hydrochloride adsorption on amino modified SBA-15 using response surface methodology. *Journal of Colloid and Interface Science* 443: 105-114.

Heikkila, T., Salonen, J., Tuura, J., Hamdy, M.S., Mul, G., Kumar, N., Salmi, T., Yu, D., Laitinen, L., Kaukonen, A.M., Hirvonen, J. & Lehto, V.P. 2007. Mesoporous silica material TUD-1 as a drug delivery system. *International Journal of Pharmaceutics* 331: 133-138.

Hong, R.Y., Li, J.H., Chen, L.L., Liu, D.Q., Li, H.Z., Zheng, Y. & Ding, J. 2009. Synthesis, surface modification and photocatalytic property of ZnO nanoparticles. *Powder Technology* 189(3): 426-432.

Irvine, J., Afrose, A. & Islam, N. 2018. Formulation and delivery strategies of ibuprofen: Challenges and opportunities. *Drug Development and Industrial Pharmacy* 44(2): 173-183.

Kamarudin, N.H.N., Jalil, A.A., Triwahyono, S., Salleh, N.F.M., Karim, A.H., Mukti, R.R., Hameed, B.H. & Ahmad, A. 2013. Role of 3-aminopropyltriethoxysilane in the preparation of mesoporous silica nanoparticles for ibuprofen delivery: Effect on physicochemical properties. *Microporous and Mesoporous Materials* 180: 235-241.

Li, J., Wang, H., Li, H., Xu, L., Guo, Y., Lu, F., Pan, W. & Li, S. 2016. Mutual interaction between guest drug molecules and host nanoporous silica xerogel studied using central composite design. *International Journal of Pharmaceutics* 498(1-2): 32-39.

Li, Y. & Yang, L. 2015. Driving forces for drug loading in drug carriers. *Journal of Microencapsulation* 32(3): 255-272.

Li, Z., Yu, L., Dong, B., Geng, F., Zheng, L. & Li, G. 2008. Synthesis and characterization of mesoporous silica templated by amphiphilic RTILs. *Journal Dispersion Science and Technology* 29: 1066-1071.

Lv, X., Zhang, L., Xing, F. & Lin, H. 2016. Controlled synthesis of monodispersed mesoporous silica nanoparticles: Particle size tuning and formation mechanism investigation. *Microporous and Mesoporous Materials* 225: 238-244.

Maleki, A., Kettiger, H., Schoubben, A., Rosenholm, J.M., Ambrogi, V. & Hamidi, M. 2017. Mesoporous silica materials: From physico-chemical properties to enhanced dissolution of poorly water-soluble drugs. *Journal of Controlled Release* 262: 329-347.

Mccarthy, C.A., Ahern, R.J., Dontireddy, R., Ryan, K.B. & Crean, A.M. 2016. Mesoporous silica formulation strategies for drug dissolution enhancement: A review. *Expert Opinion on Drug Delivery* 13(1): 93-108.

Mohamed Isa, E.D., Mahmud, I.S., Ahmad, H. & Abdul Rahman, M.B. 2019. Dependence of mesoporous silica properties on its template. *Ceramics International* 45(9): 12149-12153.

Mohamed Isa, E.D., Abdul Rahman, M.B. & Ahmad, H. 2018. Monodispersed mesoporous silica nanospheres based on pyridinium ionic liquids. *Journal of Porous Materials* 25(5): 1439-1446.

Narayan, R., Nayak, U.Y., Raichur, A.M. & Garg, S. 2018. Mesoporous silica nanoparticles: A comprehensive review on synthesis and recent advances. *Pharmaceutics* 10(3): 118.

Postnova, I.V., Jen, L. & Shchipunov, Y.A. 2013. Synthesis of monolithic mesoporous silica with a regular structure (SBA-15) and macropores in neutral aqueous solution at room temperature. *Colloid Journal* 75: 231-233.

Quevedo, G.P., Celis, A.C., Ordonez, C.V. & Martinez, M.L.O. 2018. SBA-type mesoporous materials with cylindrical and spherical structures for the controlled loading and release of ibuprofen. *Journal of Sol-Gel Science and Technology* 85(2): 486-494.

Rameli, N., Jumbri, K., Ramli, A., Wahab, R. & Huyop, F. 2018. Synthesis and characterization of mesoporous silica nanoparticles using ionic liquid as template. *Journal of Physics: Conference Series*. IOP Publishing. 012068.

Sabbagh, F. & Muhamad, I.I. 2017. Acrylamide-based hydrogel drug delivery systems: Release of Acyclovir from MgO nanocomposite hydrogel. *Journal of the Taiwan Institute of Chemical Engineers* 72: 182-193.

Saptiama, I., Kaneti, Y.V., Oveisi, H., Suzuki, Y., Tsuchiya, K., Takai, K., Sakae, T., Pradhan, S., Hossain, S.A., Fukumitsu, N., Ariga, K. & Yamauch, Y. 2018. Molybdenum adsorption properties of alumina-embedded mesoporous silica for medical radioisotope production. *Bulletin of the Chemical Society of Japan* 91(2): 195-200.

Slowing, I.I., Vivero-Escoto, J.L., Trewyn, B.G. & Lin, V.S.Y. 2010. Mesoporous silica nanoparticles: Structural design and applications. *Journal of Materials Chemistry* 20(37): 7924-7937.

Sriamornsak, P., Nunthanid, J., Cheewatanakornkool, K. & Manchun, S. 2010. Effect of drug loading method on drug content and drug release from calcium pectinate gel beads. *AAPS PharmSciTech* 11(3): 1315-1319.

Szegedi, A., Popova, M., Goshev, I. & Mihály, J. 2011. Effect of amine functionalization of spherical MCM-41 and SBA-15 on controlled drug release. *Journal of Solid State Chemistry* 184(5): 1201-1207.

Vadia, N. & Rajput, S. 2011. Mesoporous material, MCM-41: A new drug carrier. *Asian Journal of Pharmaceutical and Clinical Research* 4(2): 44-53.

Vallet-Regí, M., Colilla, M., Izquierdo-Barba, I. & Manzano, M. 2018. Mesoporous silica nanoparticles for drug delivery: Current insights. *Molecules* 23(1): 47.

Wang, Y., Zhao, Q., Hu, Y., Sun, L., Bai, L., Jiang, T. & Wang, S. 2013. Ordered nanoporous silica as carrier for improved delivery of water insoluble drugs: A comparative study between three dimensional and two dimensional macroporous silica. *International Journal Nanomedicine* 8: 4015-4031.

Ward, A.J., Pujari, A.A., Costanzo, L., Masters, A.F. & Maschmeyer, T. 2011. Ionic liquid-templated preparation of mesoporous silica embedded with nanocrystalline sulfated zirconia. *Nanoscale Research Letters* 6(1): 192.

Xie, Y., Kocaefe, D., Chen, C. & Kocaefe, Y. 2016. Review of research on template methods in preparation of nanomaterials. *Journal of Nanomaterials* 2302595.

Xu, Z., Ji, Y., Guan, M., Zhao, C. & Zhang, H. 2010. Preparation and characterization of L-Leucine-modified amphiprotic bifunctional mesoporous SBA-15 molecular sieve as a drug carrier for ribavirin. *Applied Surface Science* 256(10): 3160-3165.

Zaharudin, N.S., Mohamed Isa, E.D., Ahmad, H., Abdul Rahman, M.B. & Jumbri, K. 2020. Functionalized mesoporous silica nanoparticles templated by pyridinium ionic liquid for hydrophilic and hydrophobic drug release application. *Journal of Saudi Chemical Society* 24(3): 289-302.

Zhang, J., Ma, Y., Shi, F., Liu, L. & Deng, Y. 2009. Room temperature ionic liquids as templates in the synthesis of mesoporous silica via a sol-gel method. *Microporous and Mesoporous Materials* 119(1-3): 97-103.

*Corresponding author; email: khairulazhar.jumbri@utp.edu.my

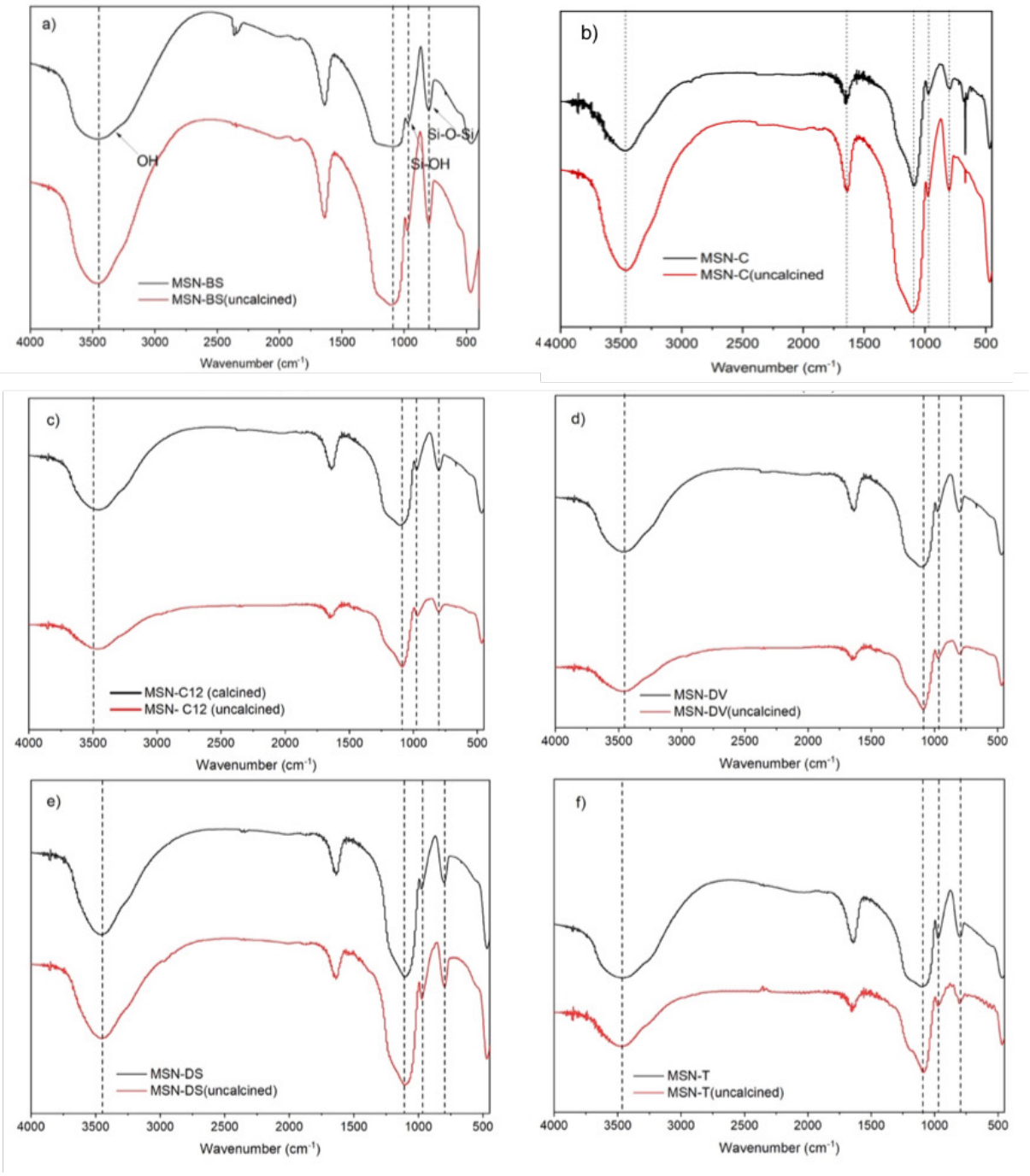

FIGURE S1. FTIR spectra of (a) MSN-BS, (b) MSN-C, (c) MSN-C12, (d) MSN-DV, (e) MSN-DS, and (f) MSN-T before and after calcination

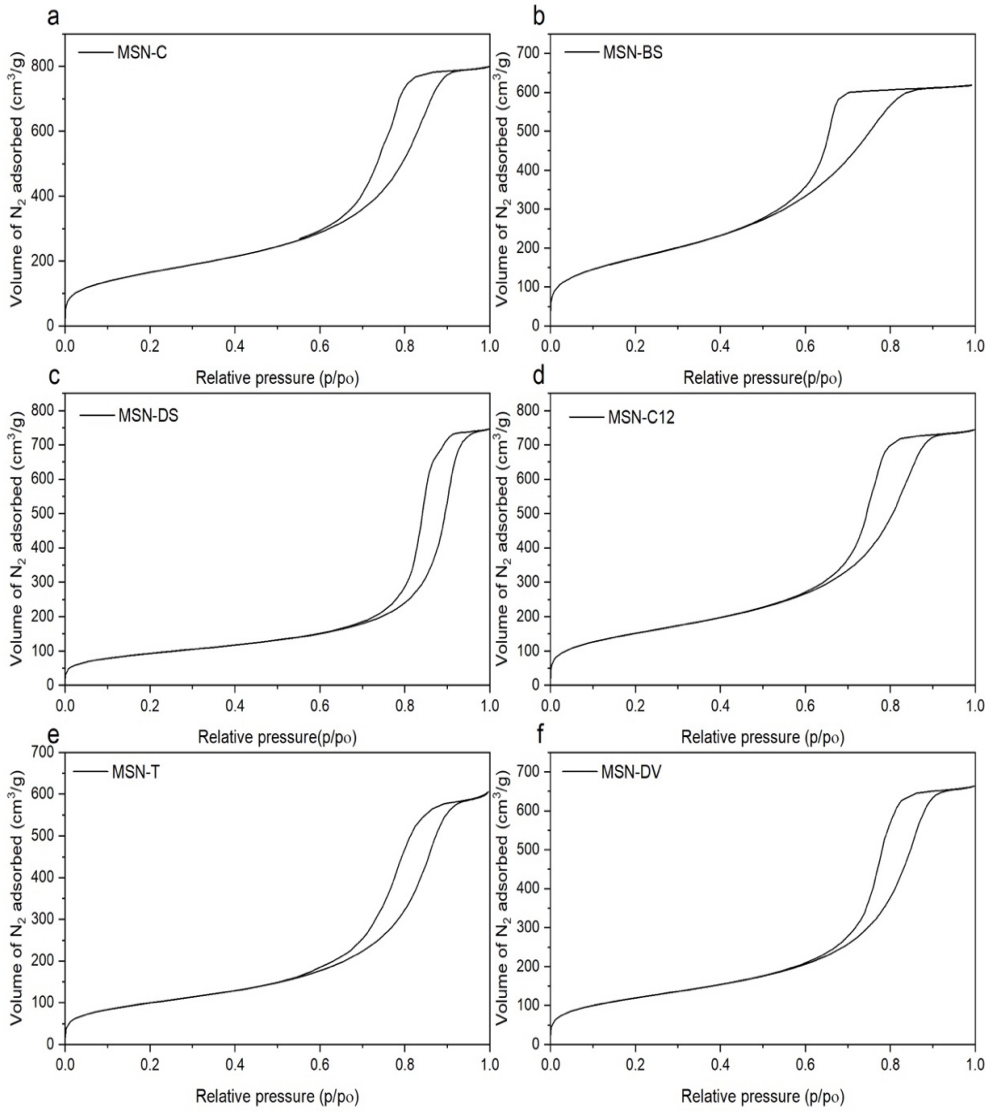

FIGURE S2. N_2 adsorption/desorption isotherm of MSN (a) MSN-C, (b) MSN-BS, (c) MSN-DS, (d) MSN-C12, (e) MSN-T, and (f) MSN-DV

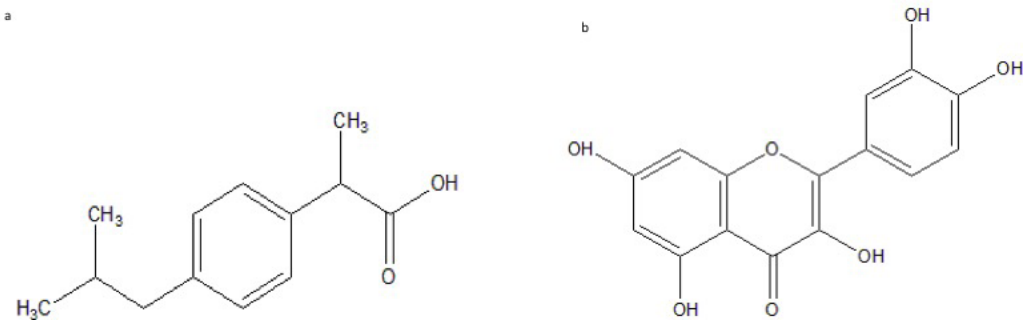

FIGURE S3. a) Ibuprofen (IBU), and b) Quercetin (QUE)

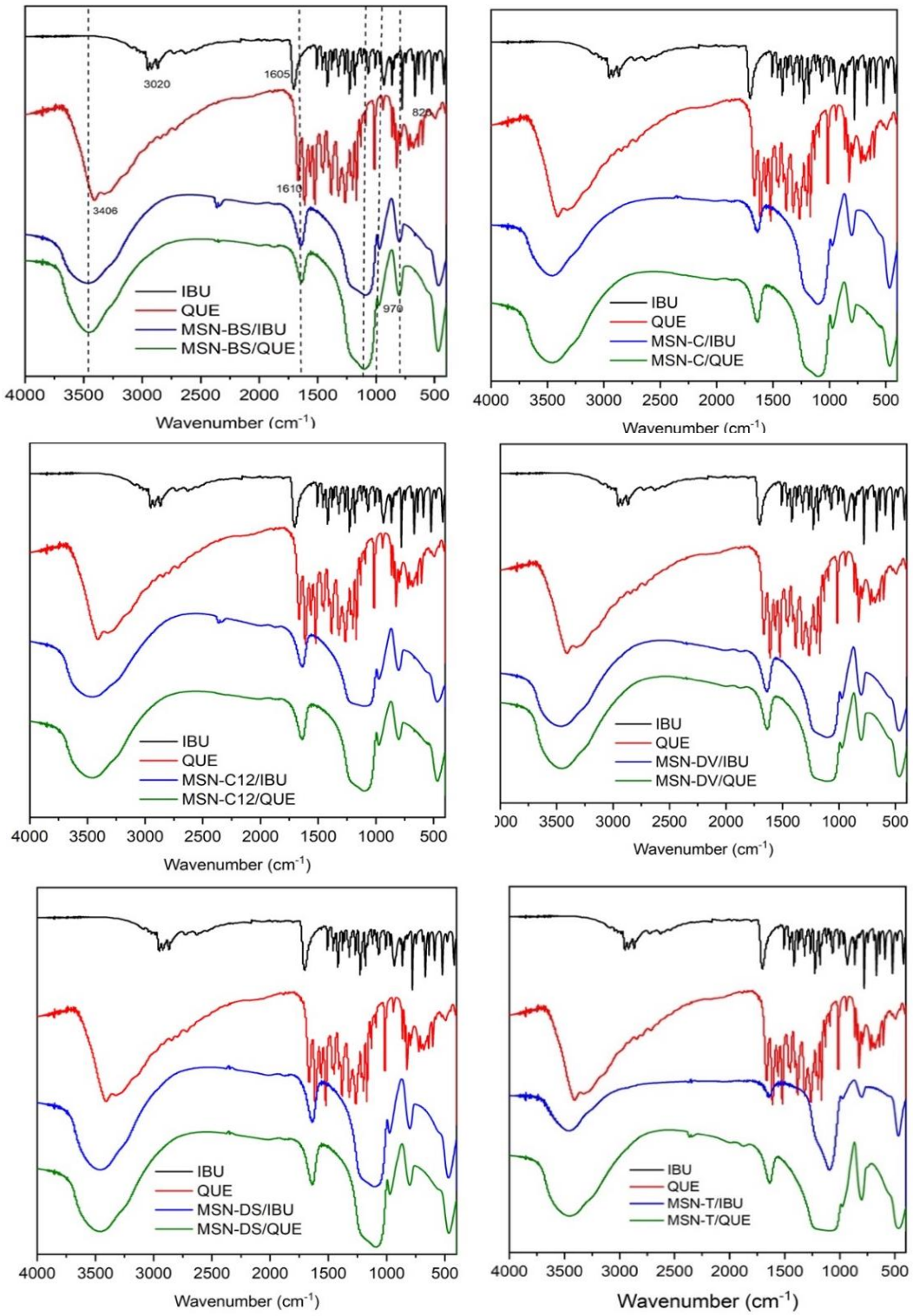

FIGURE S4. FTIR spectra of MSN-BS, MSN-C, MSN-C12, MSN-DV, MSN-DS, and MSN-T before and after drug loaded

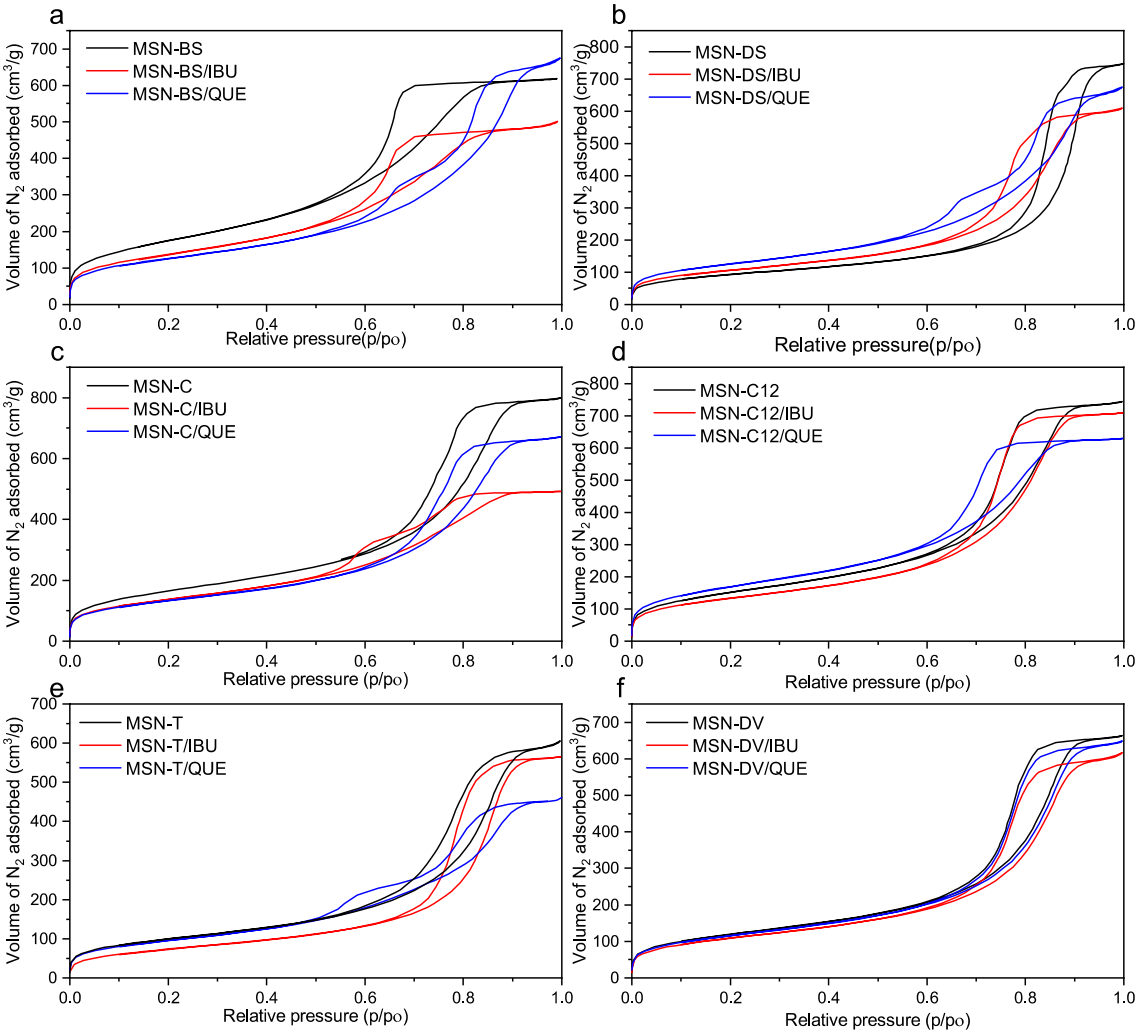

FIGURE S5. N_2 adsorption/desorption isotherm of MSN (a) MSN-C, (b) MSN-BS, (c) MSN-DS, (d) MSN-C12, (e) MSN-T, and (f) MSN-DV after drug loaded